

Analysis of a Pressure-Driven Folding Flow Microreactor with Nearly Plug-Flow Characteristics

A. Vikhansky

School of Engineering and Material Science, Queen Mary, University of London, London E1 4NS, U.K.

J. M. Macinnes

Dept. of Chemical and Process Engineering, University of Sheffield, Sheffield S1 3JD, U.K.

DOI 10.1002/aic.12129

Published online December 18, 2009 in Wiley InterScience (www.interscience.wiley.com).

We discuss the possibility of designing a pressure-driven single-phase microreactor with characteristics similar to that in an ideal plug-flow reactor. We consider equations for the moments of the residence time distribution and investigate the behavior of the solution in long spatially-periodic channels. If the microreactor consists of a large number of folding flow elements, the chaotic advection plays a double role: it mixes the chemical species and suppresses the axial dispersion. It is shown using analytical estimates and numerical modeling that chemical reactions have different sensitivity to the axial dispersion and for some reactions the effect of dispersion can be successfully eliminated. © 2009 American Institute of Chemical Engineers *AIChE J.*, 56: 1988–1994, 2010
Keywords: microfluidics, chaotic mixing, Taylor dispersion, RTD, chemical reactions

Introduction

As a viscous liquid is driven through a microfluidic device by pressure difference, some of the liquid spends more time in the device than others as a result of the nonslip condition at the bounding walls. This phenomenon which is known as Taylor dispersion^{1–3} or the residence time distribution (RTD)^{4–6} significantly limits the effectiveness of microfluidic devices.^{4,7} It has been realised recently that chaotic advection introduced by mixing elements provides a partial solution to the problem.^{8–10} Recent progress in the microfluidic technology has turned the research's attention to the RTD in the microdevices, usually operated under laminar regimes.^{11–15}

Although some dispersion is unavoidable, it can be significantly suppressed by proper design of the mixer element and its effect on the outcome of chemical reactions occurring in

the flow can be effectively controlled. In Section 2, we discuss the Taylor dispersion in a microdevice consisting of series of identical elements. The equations of the moments of the RTD are obtained and the structure of the solution of these equations in spatially-periodic channels is considered. Section 3 describes the effect of the dispersion on the outcome of chemical reactions and formulates general requirements for the number of elements and the pressure drop.

Dispersion in spatially-periodic channels

Consider the steady flow of a viscous incompressible liquid through a channel with space-periodic geometry. The velocity and pressure fields are determined by the Navier-Stokes equations:

$$\rho \vec{u} \cdot \nabla \vec{u} = -\nabla p + \mu \nabla^2 \vec{u} \quad \text{and} \quad \nabla \cdot \vec{u} = 0 \quad (1)$$

where \vec{u} is the velocity, ρ is the fluid density, μ is the dynamic viscosity and p is the pressure.

Correspondence concerning this article should be addressed to A. Vikhansky at a.vikhansky@qmul.ac.uk

The flow carries m species, which undergo n chemical reactions. The advection-diffusion-reaction equations are:

$$\vec{u} \cdot \nabla C_i - D \nabla^2 C_i = \sum_{j=1}^n v_{ij} Y_j(C), \quad (2)$$

where C_i is the concentration of species i ($i = 1, m$), D is the coefficient of molecular diffusivity, v_{ij} is a stoichiometric coefficient (with appropriate sign) for the i th component in the j th reaction and Y_j is reaction rate (in mole/m³s) of the j th reaction. The walls are impermeable for the species, i.e., the normal derivative of the concentration at the walls $\partial_n C_i$ is zero. Even if the mixer is operated in the Stokes regime and the LHS in Eq. 1 can be neglected, the convection term in Eq. 2 is not negligible since the Schmidt number, $Sc = \mu/(\rho D)$, is typically of order 10³.

We are mainly interested in systems with low diffusivity and high Péclet number, $Pe = dU/D$, where d is channel's width and U is characteristic velocity of the fluid. It is known that a low diffusivity impairs the performance of a reactor in two ways: it leads to poor and slow mixing and widens the distribution of residence times.¹ Chaotic advection offers a solution for both of these difficulties,^{8–10,13–18} and our task is to investigate whether this approach can be effective in practice. Although the results presented below hold for any chaotic micromixer with spatially periodic geometry, we will look quantitatively at particular element geometry: a folding flow micromixer operated under Stokes conditions.¹⁵ The schematic view of the mixer is presented in Figure 1. Two elements are shown, each serving to split the flow and then recombine it such that (approximately) the interface area between two initially segregated streams is doubled and the striation thickness is halved. So, a single step achieves an approximation of the baker's transformation.^{15–18}

The volume and length of each element of the channel are V_0 and l_0 , respectively. The mean residence time of the liquid inside the element and the mean velocity can be defined as follows:

$$\tau_0 = V_0/Q_0 \quad \text{and} \quad U = l_0/\tau_0,$$

where Q_0 is the volume flow rate. If the channel consists of N elements and has total length $L = Nl_0$, the mean residence time of the liquid in the channel is as follows:

$$\tau_R = N\tau_0 = L/U.$$

As the flow field is nonuniform, some liquid parcels spend more and some less than the mean time in the mixer. This phenomenon results in what is known as axial (or Taylor) dispersion.^{1–3} The concentration of a passive scalar at the inlet of the mixer affects the concentration at the outlet through the RTD as follows:

$$C_{\text{out}}(t, L) = \int_0^\infty E(\tau) C_{\text{in}}(t - \tau, 0) d\tau. \quad (3)$$

This formula constitutes the mathematical definition of the RTD $E(\cdot)$.^{4,5}

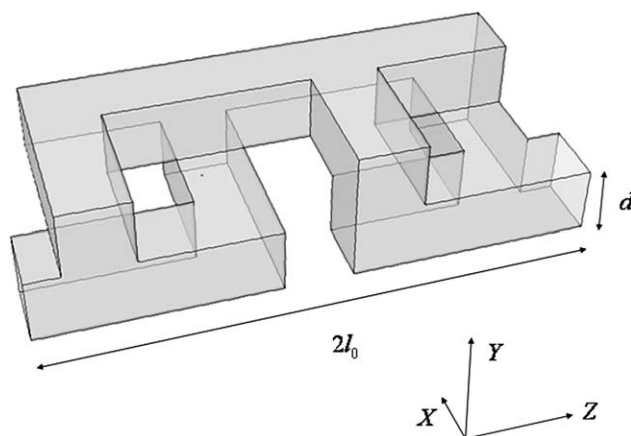


Figure 1. Schematic view of two periodic elements of the mixer: dimensions and the coordinate axis.

There are two numerical methods which allow investigation of axial dispersion: the Monte Carlo (MC) particle tracking method and the method based on solution of auxiliary equations.^{9,19} Using the particle tracking method, we are tracking a massless particle, which is advected by the flow and undergoes Brownian motion, i.e., we solve the following stochastic differential equation for a particle position \vec{x} :

$$d\vec{x} = \vec{u}dt + \sqrt{2D}d\vec{W} \quad (4)$$

where $d\vec{W}$ is an increment of a Wiener process with unit dispersion, and register the time spent by the tracer in the channel element.

The second method is more involved. Consider the ages of different particles: when a particle enters the channel its age s is 0 and then increases as $\dot{s} = l$. Denote the probability that a particle at point \vec{x} has age between s and $s + ds$ as $P(\vec{x}; s)ds$. Obviously, RTD $E(s)$ can be expressed as flux-averaged $P(\vec{x}; s)$ over the outlet A

$$E(s) = \int_A P(\vec{x}, s) u_n dA \Big/ \int_A u_n dA. \quad (5)$$

As a particle undergoes advection and diffusion in the three-dimensional physical space as well as advection with unit velocity along the s -axis, the equation for the probability density function (PDF) $P(\vec{x}; s)$ reads:

$$\vec{u} \cdot \nabla P - D \nabla^2 P = -\partial P / \partial s, \quad (6)$$

The boundary conditions are the same as in Eq. 2.

We introduce the following transformation of the variables:

$$s = \frac{z}{U} + \theta, \quad \frac{\partial}{\partial s} = \frac{\partial}{\partial \theta}, \quad \frac{\partial}{\partial z} = \frac{\partial}{\partial z} - \frac{1}{U} \frac{\partial}{\partial \theta}. \quad (7)$$

Substitution of Eq. 7 into Eq. 6 yields:

$$\vec{u} \cdot \nabla P - D \nabla^2 P = -w \frac{\partial P}{\partial \theta} - D \left[\frac{1}{U} \frac{\partial^2 P}{\partial z \partial \theta} - \frac{1}{U^2} \frac{\partial^2 P}{\partial \theta^2} \right], \quad (8)$$

where

$$w = \frac{U - u_z}{U} \quad (9)$$

is the deviation of the axial velocity from its mean value U . Multiplying Eq. 8 by θ^m and integrating one can obtain the following equations for the moments of the PDF:

$$\vec{u} \cdot \nabla \theta_m - D \nabla^2 \theta_m = m w \theta_{m-1} + m D \left[\frac{1}{U} \frac{\partial \theta_{m-1}}{\partial z} + \frac{(m-1)}{U^2} \theta_{m-2} \right], \quad (10)$$

where $\theta_m = \int \theta^m P d\theta$ and θ_m is 0 for negative m . It is known² that the second term in the source term of Eq. 10 provides only $O(\text{Pe}^{-2})$ contribution to the Taylor dispersion coefficient. As we are interested in systems with low diffusivity, the second term in the source term of Eq. 10 can be neglected. Our numerical data justifies this assumption. Starting from the obvious result $\theta_0 = 1$, these equations can be, in principle, solved for higher moments giving the complete solution of the problem. Although the chaotic nature of the flowfield makes this problem almost as difficult as the solution of Eq. 2, some conclusions can be reached about the structure of the solution of Eq. 10 without solving it.

We denote the averaging over one element of the mixer as

$$\langle \phi \rangle = \frac{1}{V_0} \int_{V_0} \phi dV.$$

Consider the equation for the first moment:

$$\vec{u} \cdot \nabla \theta_1 - D \nabla^2 \theta_1 = w, \quad (11)$$

Equation 9 implies that the source term of Eq. 11 averaged over an element of the mixer is equal to zero. This means that there exists a periodic solution along the z -axis such that $\langle \theta_1 \rangle = 0$, i.e., a pulse of the solute introduced at the inlet propagates downstream with velocity U .

To proceed further we need to consider the following problem:

$$\vec{u} \cdot \nabla \varphi - D \nabla^2 \varphi = f, \quad (12)$$

where $\langle f \rangle = 0$ and the flux of φ across the walls of the mixer is 0. If we denote a solution of the above problem such that $\langle \varphi \rangle = 0$ as $Y(f)$, the solution of Eq. 11 reads: $\theta_1 = Y(w)$. As we have seen, the mean value of the RHS of Eq. 11 is 0, therefore, θ_1 is periodic along the z -axis. If we substitute θ_1 into the equations for the second moment, the RHS of the corresponding equation is not zero and there is no periodic solution for θ_2 . Therefore, θ_2 must be split into two parts: $\theta_2 = \theta'_2 + \beta_2 z$, where $\langle \theta'_2 \rangle = 0$ is a periodic part and β_2 is the mean gradient of the second moment along the channel. Equation for θ' reads:

$$\vec{u} \cdot \nabla \theta'_2 - D \nabla^2 \theta'_2 = -u_z \beta_2 + 2w \theta_1, \quad (13)$$

To satisfy the solvability condition for Eq. 13, we require that the mean value of the RHS is zero. Therefore:

$$\beta_2 = 2 \langle w \theta_1 \rangle / U. \quad (14)$$

Solution for θ'_2 reads

$$\theta'_2 = Y(-u \beta_2 + 2w \theta_1). \quad (15)$$

Acting in the same manner, i.e., splitting the solution of Eq. 10 into the z -periodic and z -varying parts and applying Eq. 14, we can make some useful qualitative conclusions about the behavior of the higher moments of the RTD. The solution for the third moment reads:

$$\theta_3 = 3 \beta_2 z \theta_1 + \beta_3 z + \theta'_3, \quad (16)$$

where

$$\beta_3 = 3/U \langle w \theta'_2 - \beta_2 u_z \theta_1 \rangle, \quad (17)$$

$$\theta'_3 = Y(3w \theta'_2 - \beta_3 u_z - 3 \beta_2 u \theta_1). \quad (18)$$

The fourth moment is given by the following formulas:

$$\theta_4 = 3(\beta_2 z)^2 + \beta_4 z + z \theta'_4 + \theta''_4, \quad (19)$$

$$\theta'_4 = Y(12 \beta_2 w \theta_1 + 4 \beta_3 w - 6 \beta_2^2 u_z) \quad (20)$$

$$\beta_4 = 1/U \langle 4w \theta'_3 - u_z \theta'_4 \rangle, \quad (21)$$

$$\theta''_4 = Y(4w \theta'_3 - u_z \theta'_4 - \beta_4 u_z). \quad (22)$$

Therefore, the skewness $Sk = \theta_3/\theta_2^{3/2}$ and the kurtosis $Ku = \theta_4/\theta_2^2 - 3$ averaged over an element of the mixer scale as $\langle Sk \rangle = (\beta_3 z)/(\beta_2 z)^{3/2} \sim z^{-1/2}$ and $\langle Ku \rangle = (\beta_4 z)/(\beta_2 z)^2 \sim z^{-1}$. As the length of the mixer tends to infinity, Sk and Ku approach 0 and the shape of the pulse of the concentration is Gaussian with standard deviation $\beta_2 z$.

According to (14) the standard deviation of the residence time in the whole channel (averaged over the last element of the mixer) is $\sigma_R^2 = \beta_2 L$. It can be rewritten as

$$\sigma_R^2 = \beta_2 L = \frac{2LD_T}{U^3},$$

where $D_T = U^3 \beta_2 / 2$ is the Taylor dispersion coefficient, i.e., the apparent diffusivity along the channel.^{1-3,5} Finally, the above formula yields after some algebra:

$$\sigma_R^2 = \beta_2 L = \frac{2LD_T}{U^3} = \frac{2}{N} \frac{D_T}{U l_0} \tau_R^2 = \frac{\alpha_2^2}{N} \tau_R^2, \quad (23)$$

where

$$\alpha_2^2 = 2 \frac{D_T}{l_0 U} = \frac{\beta_2 l_0}{\tau_0^2} \quad (24)$$

is a dimensionless coefficient. If one denotes the standard deviation of the time spent by a particle in a single element of the channel as σ_0 , then α_2 can be interpreted as the ratio of the

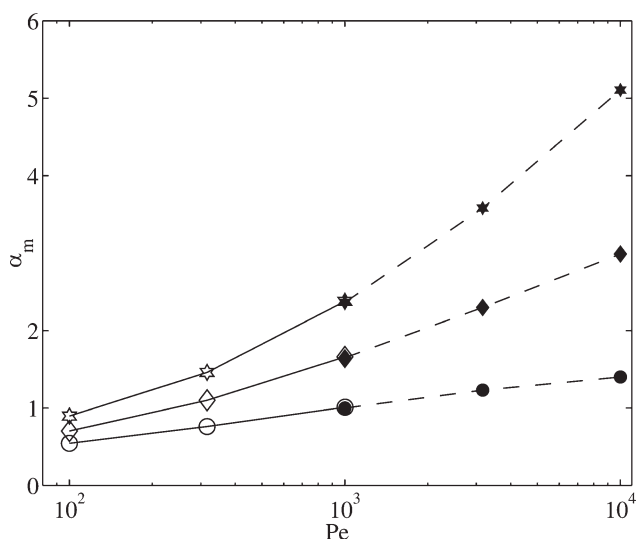


Figure 2. Parameters α_2 (circles), α_3 (diamonds) and α_4 (stars), as a function of Pe calculated by the finite-difference method (open symbols, solid lines) and by the Monte Carlo method (bold symbols, dashed lines).

standard deviation to the mean residence time for passage through a single element: $\alpha_2 = \sigma_0/\tau_0$. In the same manner, we can define the corresponding constants for the higher moments:

$$\alpha_m^m = \frac{\beta_m l_0}{\tau_0^m} = \frac{\beta_m L}{\tau_R^m} N^{m-1} \quad (25)$$

Under Stokes flow conditions, α_2 is a function of the geometry and Péclet number. According to Eq. 11 θ_1 can be viewed as a passive scalar which is supplied to the system at scales of order d by a source of intensity $(U - u_z)/U$ having zero mean and then dissipated by diffusion. In a chaotic flow with high Pe , the dissipation occurs at scales much smaller than the main scale of the flow. As $u_z(x,y,z)$ is a smooth function, the contribution of small scales to the product $\langle w\theta_1 \rangle$ in Eq. 14 is small, and we can expect that in a chaotic flow α_2 does not depend strongly on Pe . Inspection of Eqs. 12 and 13 shows that the same arguments can be applied to evolution of the auxiliary variables θ_i' and, finally, to the coefficients α_i . Our theoretical analysis and numerical experiments with a model chaotic channel flow show a nearly logarithmical dependence of α_2 on the Pe and a very weak increase of α_i ($i > 2$) with Péclet number for a wide range of Pe .⁹

In Figure 2, we present results of the calculations of α_i for the folding flow micromixer. The flow field and the corresponding pressure drop along the channel have been calculated by a Lattice-Boltzmann (LB) method.²⁰ The calculations of α_i are performed by the MC method and according to Eqs. 11–22. Unfortunately, the range of Péclet number accessible to both methods is limited. The increment of the mesh which is necessary to keep the numerical diffusion in Eq. 10 lower than the physical diffusion scales as Pe^{-1} , which makes a finite-difference method very time-consuming

for high Pe . When MC stochastic particles tracking method is used, the tracers can stack in a corner or in a “lens” with numerically negative velocity divergence. If the diffusivity is strong enough, the tracer leaves these regions quickly due to the Brownian motion and the overall result is not significantly distorted. If the stochastic term in Eq. 4 is small, the small numerical errors in the flow field cause large errors in the calculations of residence time. However, both methods give the same results (for the corresponding values of Pe). Note that while we have neglected terms of order D in the RHS of Eq. 10, the MC method is accounting for the neglected terms. Therefore, the numerical data justifies our assumptions. Although the available range of the Péclet numbers is rather limited to make quantitative conclusions, it is found that the results for this folding flow mixer are similar to those for a model chaotic channel flow.⁹

After substitution of Eq. 25 into Eqs. 16–24 the skewness and the kurtosis of the RTD can be expressed as

$$Sk = \left(\frac{\alpha_3}{\alpha_2}\right)^3 N^{-1/2}, \quad Ku = \left(\frac{\alpha_4}{\alpha_2}\right)^4 N^{-1}, \quad (26)$$

and the numbers in Figure 2 suggest that the RTD is significantly distorted along hundreds of mixer elements. The deviation of the RTD from a Gaussian distribution is strongest for high Pe . It has been shown in⁹ that at high Péclet numbers some liquid parcels spend much more time than the average in the mixer due to the vanishingly small advection near the channel’s walls.

According to Eq. 23, increasing the number of elements (and correspondingly miniaturising the mixer) reduces the axial dispersion. On the other hand, as $\sigma_R/\tau_R = \alpha_2 N^{-1/2}$ and α_2 is around unity, creation of a very narrow RTD, say 1% of mean residence time, requires a mixer consisting of thousands of mixing elements. This severe limitation becomes more obvious if one considers the pressure drop required to drive the fluid through the channel. The pressure drop along a single element is as follows¹⁵:

$$\Delta p_0 = \gamma \mu / \tau_0, \quad (27)$$

where γ is a dimensionless coefficient. Our LB results show that for the folding flow mixer considered in this work $\gamma = 1190$. After some algebra Eqs. 23 and 27 yield the following expression for pressure drop in a chain consisting of N elements:

$$\Delta p = \gamma N \frac{\mu}{\tau_0} = \gamma N^2 \frac{\mu}{\tau_R} = \gamma \alpha_2^4 \left(\frac{\tau_R}{\sigma_R}\right)^4 \frac{\mu}{\tau_R}. \quad (28)$$

The mean residence time $\tau_R \sim \tau_C$, where τ_C is the characteristic time for a reaction. Therefore, while the ratio σ_R/τ_R decreases as $N^{-1/2}$, the pressure drop grows as N^2 and although some reduction of the axial expression by the chaotic mixing is possible, the cost of the improvement rises very quickly. For example, for a liquid reaction in aqueous solution where $\tau_C = 10$ s one can reach $\sigma_R/\tau_R = 0.1$ with $N \sim 100$ and pressure drop about 10^3 Pa, which can be easily achieved. But an attempt to reduce the axial dispersion to very small levels faces significant difficulties: achieving

$\sigma_R/\tau_R \approx 10^{-2}$, for example, requires about 10^4 mixing elements and $\Delta p \approx 100$ Bar, which although possible pushes into an inconvenient range of pressure drop.

It might be of interest to compare the performance of the folding flow micromixer with a straight channel. The pressure drop in a cylindrical channel with the same length (i.e., $l_0 = 4d$) is as follows:

$$\Delta P = \frac{32\mu l_0 U}{d^2} = 512 \frac{\mu U}{l_0} = 512 \frac{\mu}{\tau_0}$$

and the coefficient of Taylor dispersion is as follows:

$$D_T = \frac{Pe}{192} U d.$$

Therefore, for the cylindrical channel $\gamma = 512$ and $\alpha_2^2 = Pe/384$. Eq. 23 shows that for $Pe \approx 400$ the folding flow mixer provides the same σ_R as the straight channel, whereas Eq. 29 implies that the folding flow mixer requires the same ΔP at $Pe \approx 600$. To achieve the same value of σ_R at $Pe \approx 10^4$, the cylindrical channel has to be more 10 times longer than the flow folding mixer and requires approximately 100 times higher pressure drop than the folding flow micromixer. Note that the typical microchannels have a shallow profile^{11,12} and have higher pressure drop and higher coefficients of Taylor dispersion than the cylindrical channel, then the effect of chaotic mixing on the RTD becomes even more pronounced.

Certainly, the mixer geometry considered in this work is not optimal: avoiding sharp corners can reduce both α_2 and γ . However, Eq. 11 shows that the deviations in residence time are generated by the nonuniformities of the axial velocity, which will in all cases be of order U and this cannot be significantly changed due to the non-slip boundary conditions at the walls of the channel. The decay of θ_1 depends on the mixing properties of the flow, but all elements of folding flow type have similar mixing characteristics, i.e., one period of the flow approximates the baker's transformation.¹⁸ Therefore, the estimates given in the present work, although based on one particular example, give estimation about performance of a wide variety of pressure-driven micromixers.

Effect of the dispersion on the chemical reactions

Although our analysis shows that design of a pressure-driven mixer to approach plug flow characteristics is severely limited by pressure drop, the results contain a germ of optimism too. This is because the acceptable level of axial dispersion in the reactor depends on the nature of the chemical reaction. Consider the first order reaction under perfect plug flow conditions:

$$dC/dt = -C/\tau_C, \quad C(t) = C_0 \exp(-t/\tau_C) \text{ and} \\ C_b = C_0 \exp(-\tau_R/\tau_C), \quad (29)$$

where C_0 , C_b are initial concentration and the concentration at the end of the process. The mean concentration at the outlet is $\int C(t)E(t)dt$.⁵ To characterize the effect of the axial dispersion on the yield of the reaction, we introduce the following function:

$$\varepsilon = \int \left(\frac{C(t)}{C_b(\tau_R)} - 1 \right) E(t) dt \equiv \overline{\left(\frac{C(t)}{C_b(\tau_R)} - 1 \right)}, \quad (30)$$

which is the relative deviation of the yield of the reaction in the pressure-driven mixer in comparison to the ideal plug-flow conditions.

To evaluate the above integral, we represent t as $t = \tau_R + t'$ and expand the exponentials into Taylor series. Therefore

$$\begin{aligned} \overline{\left(\frac{C}{C_b} - 1 \right)} &= \overline{\left(\frac{\exp(-t/\tau_C)}{\exp(-\tau_R/\tau_C)} - 1 \right)} \\ &\approx \frac{1}{2} \frac{\alpha_2^2}{N} \left(\frac{\tau_R}{\tau_C} \right)^2 - \frac{1}{6} \frac{\alpha_3^3}{N^2} \left(\frac{\tau_R}{\tau_C} \right)^3 + \frac{1}{24} \left(3 \frac{\alpha_2^4}{N^2} + \frac{\alpha_4^4}{N^3} \right) \left(\frac{\tau_R}{\tau_C} \right)^4 + \dots \end{aligned} \quad (31)$$

where $\tau_R/\tau_C = \ln(C_0/C_b)$.

For $C_0/C_b = 10^2$ the second and third terms in the above expansion are negligible when $N \geq 100$ and only the first term is relevant for our analysis. If our aim is to keep the integral ε as low as 1%, we need about then 10^3 elements for $Pe = 10^3$ and about 4×10^3 elements for $Pe = 10^4$. The corresponding pressure drops for aqueous solution are 1 Bar and 16 Bar, respectively. Note that many applications, for example, chemical kinetics experiments, require lower values of C_0/C_b and, therefore, lower numbers of elements and lower pressure drops.

Similar analysis can be applied to the following second order reaction:

$$dC/dt = -kC^2, \quad \text{and} \quad 1/C(t) - 1/C_0 = kt, \quad (32)$$

where k is the constant of the reaction. For long enough times $C = C_0$ and the second of Eq. 32 reads $C(t) \approx 1/kt$. Therefore, an estimate can be made⁵:

$$\begin{aligned} \varepsilon &\approx \overline{\left(\frac{k\tau_R}{k(\tau_R + t')} - 1 \right)} = \overline{\frac{1}{1 + t'/\tau_R}} \\ &\approx \overline{\left(\frac{t'}{\tau_R} \right)^2} - \overline{\left(\frac{t'}{\tau_R} \right)^3} + \overline{\left(\frac{t'}{\tau_R} \right)^4} + \dots = \frac{\alpha_2^2}{N} - \frac{\alpha_3^3}{N^2} + 3 \frac{\alpha_2^4}{N^2} + \frac{\alpha_4^4}{N^3} \end{aligned} \quad (33)$$

and between 100 and 400 elements are sufficient to have $\varepsilon = 10^{-2}$ for $Pe = 10^3 - 10^4$. As in the previous example, for $N \geq 100$ the first term of the expansion (33) is significantly larger than other terms.

Note that for characteristic width of the channel d is about $10^2 \mu m$, the Reynolds number based on the residence time in a single element of the mixer is $Re = \rho d^2 / (\mu \tau_0) = \rho d^2 N / (\mu \tau_R)$ and therefore for water $Re \approx 1$ and the flow is in the Stokes regime as was assumed at the beginning.

For a general reaction scheme, we replace Eq. 2 with the following one-dimensional equation along the z -direction:

$$\partial_z \bar{C}_i - Pe_T^{-1} \partial_z^2 \bar{C}_i = \sum_{j=1}^n \nu_{ij} Y'_j(\bar{C}), \quad (34)$$

where \bar{C} is the concentration averaged over one element of the channel, $Pe_T = UL/D_T$ is the Péclet number based on the Taylor dispersion coefficient and the length of the reactor, i.e., while Pe characterises the micromixing, Pe_T characterises the

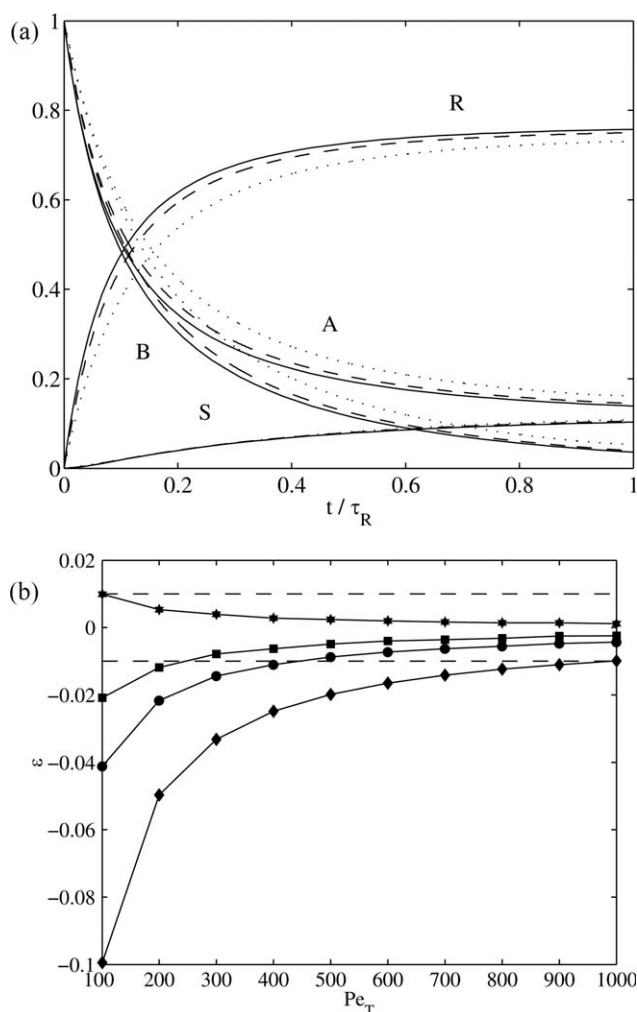


Figure 3. Distribution of species concentrations along the mixer. Solid lines: $Pe_T = \infty$ (plug flow); dashed lines: $Pe_T = 100$; dotted lines: $Pe_T = 20$ (a) and relative error ϵ_C for $C \equiv A$ (circles), B (diamonds), R (stars), S (squares) as a function of Pe_T .

The dashed lines correspond to the $\epsilon_C = \pm 10^{-2}$ band (b).

micromixing in the entire channel; Y'_j is the dimensionless reaction rate. Note that Eq. 34 reproduces correctly only the second moment of the RTD, but as we have seen earlier the contribution of higher moments of the RTD to the yield of the reaction is negligible if the mixer is long enough. Certainly, this assumption holds only for the given range of the Péclet numbers. Under higher values of Pe the deviation of the RTD from the Gaussian shape is stronger and the chemical reaction in the near-wall zones may affect the performance of the entire reactor.

To justify the replacement of C by \bar{C} in Eq. 34 and the corresponding replacement of $Y'_j(C)$ by $Y'_j(\bar{C})$, we need to consider how quickly the fluctuations of the concentration are dissipating due to the chaotic mixing. It is known that from 10 to 20 mixing elements are sufficient to completely mix two initially separated streams.¹⁵ As the mixer consists of hundreds of the elements, one can expect that the charac-

teristic mixing time is much shorter than the reaction time and the replacement of $Y'_j(C)$ by $Y'_j(\bar{C})$ should not cause a significant error. A more precise analysis is as follows. The generation rate of the fluctuations due to the axial dispersion and decay rate of the fluctuations c' due to the mixing are as follows²¹

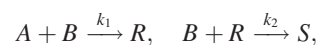
$$2D_T(\partial_z \bar{C})^2 \quad \text{and} \quad 2\lambda c'^2/\beta, \quad (35)$$

respectively, where λ is the Lyapunov exponent and β is an empirical constant, which depends on Pe (based on molecular diffusivity). Since the folding flow micromixer aims to approximate the baker's transformation, we estimate the Lyapunov exponent as $\lambda \approx \ln(2)/\tau_0$. The constant β for $Pe = 10^2 - 10^{10}$ varies between the values 3 and 5.²¹ From Eq. 23 $D_T = \alpha_2^2 U l_0/2$ and the gradient of the mean concentration can be expressed through the characteristic reaction time as $\alpha_z \bar{C} \approx \bar{C}/(\tau_C U)$. Equating the generation rate to the dissipation rate yields after some algebra:

$$\frac{c'}{\bar{C}} \approx \alpha_2^2 \frac{l_0}{\tau_C U} = \alpha_2^2 \sqrt{\frac{\beta}{2 \ln(2)}} \frac{\tau_0}{\tau_C}. \quad (36)$$

Since during the time τ_C the liquid passes through tens of the mixer's elements and, therefore, $\tau_0/\tau_C \ll 1$, we can neglect the effect of the fluctuations on the reaction rate.

As an example we consider the competitive-consecutive reaction^{5,22}



with $k_1 = 10$, $k_2 = 1$. In this case the outcome of the reaction is sensitive to the mixing rate.²² In Figure 3(a) we show the distribution of the species along the channel and compare it to the results for a plug-flow mixer. As one can see (Figure 3b), the effect of the axial dispersion is significant for $Pe_T \leq 10^2$, which corresponds to a mixer containing tens of elements, as N becomes of order 10^2 and higher, the results approach those of ideal plug-flow. For design purposes we plot the relative error

$$\epsilon_C = C(\tau_R)/C_b(\tau_R) - 1$$

for different species as a function of Pe_T in Figure 3b. The sensitivity of the error to the axial dispersion is different for the different species. If our aim is to keep ϵ_C below 10^{-2} for every species, the axial Péclet number must exceed $Pe_T = 10^3$. From Eq. 23 the number of elements is

$$N = \alpha_2^2 Pe_T/2, \quad (37)$$

and for $Pe = 10^4$ $N \approx 2 \times 10^3$. From Eq. 27 the necessary pressure drop for a liquid reaction in water ($\tau_C \sim 10$ s, $\mu \approx 10^{-3}$ kg/(m·s)) in the folding flow micromixer is about 4 Bar. Note that the high relative error for ϵ_A and ϵ_B are due to the fact that these species are consumed during the reaction and thus even a small absolute error gives large relative errors. If we are interested in minimisation of the relative errors only for the products of the reaction, the necessary number of mixing elements, and the required pressure drop can be reduced by factors 4 and 16, respectively.

Conclusions

Our analysis shows that design of a pressure driven micro-mixer with characteristics similar to the ideal plug-flow reactor is an achievable task. Although the mixer considered above is operated under Stokes conditions, the result holds for cases when inertia is not negligible. Chaotic mixing plays a double role: it mixes the chemical species and also suppresses axial dispersion. Although creation of an extremely narrow Gaussian RTD requires a high pressure drop and a large number of mixing elements, in the case of chemical reacting flow these requirements can be significantly relaxed depending on the type of the reaction. Different reactions have different sensitivity to the axial dispersion and for some reactions nearly plug-flow performance of the reactor is possible.

The performance of each element of the micromixer can be characterised by two parameters which depend on the mixer geometry: the friction coefficient γ and α_2 , which is the ratio of the standard deviation to the mean residence time in one element. Although the RTD is far from being Gaussian, for the given range of Péclet numbers, the higher moments do not play a significant role. However, one might expect that for the higher values of Pe the higher moments of the RTD are not negligible and it is important to have a reliable estimate for these moments and the effect they have on the yield of the reaction.

It is shown that the required number of elements scales as α_2^2 and the pressure drop under Stokes conditions as α_2^4 . Although the parameters γ and α_2 cannot be greatly reduced, even a small decrease in α_2 can significantly improve the performance of the micromixer. As the particular folding flow micromixer geometry analyzed in this work has been selected for simplicity and not optimum performance, refining mixer element geometry may well allow considerable improvement to be achieved.

Notation

D_T = Taylor coefficient of dispersion
 Ku = kurtosis
 l_0 = Length of an element
 L = Length of the mixer
 N = Number of elements
 Sk = Skewness
 Q_0 = Flow rate
 V_0 = Volume of an element
 U = Mean velocity

Greek letters

α_m = Dimensionless coefficients showing the growth rate of the corresponding moments of the RTD
 σ_R = Standard deviation of the residence time

θ_m = Moments of the RTD

τ_0 = Mean residence time of the liquid inside the element

τ_R = Mean residence time of the liquid in the channel

Literature Cited

1. Taylor GI. Dispersion of soluble matter in solvent flowing through a tube. *Proc R Soc Lond A*. 1953;219:186–203.
2. Aris R. On the dispersion of a solute in a fluid flowing through a tube. *Proc R Soc Lond A*. 1956;235:67–77.
3. Rosencrans S. Taylor dispersion in curved channels. *SIAM J App Math*. 1997;5:1216–1241.
4. Danckwerts PV. Continuous flow systems. *Chem Eng Sci*. 1953;2:1–13.
5. Levenspiel O. *Chemical Reaction Engineering*. New York:Wiley, 1972.
6. Rawatlal R, Starzak M. Unsteady-state residence-time distribution in perfectly mixed vessels. *AIChE J*. 2003;49:471–484.
7. Cozewith C, Squire KR. Effect of reactor residence time distribution on polymer functionalization reactions. *Chem Eng Sci*. 2000;55:2019–2029.
8. Stroock AD, Dertinger SKW, Ajdari A, Mezic I, Stone HA, Whitesides GM. Chaotic mixer for microchannels. *Science*. 2002;295:647–651.
9. Vikhansky A. Effect of diffusion on residence time distribution in chaotic channel flow. *Chem Eng Sci*. 2008;63:1866–1870.
10. Cantu-Perez A, Barrass S, Gavrilidis A. Residence time distributions in microchannels: Comparison between channels with herringbone structures and a rectangular channel. *Chem Eng J*. In Press.
11. Ajdari A, Bontoux N, Stone HA. Hydrodynamic dispersion in shallow microchannels: the effect of cross-sectional shape. *Anal Chem*. 2006;78:387–392.
12. Vikhansky A. Taylor dispersion in shallow micro-channels: aspect ratio effect. *Microfluid Nanofluid*. 2009;7:91–95.
13. Hassell DG, Zimmerman W. Investigation of the convective motion through a staggered herringbone micromixer at low Reynolds number conditions. *Chem Eng Sci*. 2006;61:2977–2985.
14. Adeosun JT, Lawal A. Numerical and experimental studies of mixing characteristics in a T-junction microchannel using residence-time distribution. *Chem Eng Sci*. 2009;64:2422–2432.
15. MacInnes JM, Vikhansky A, Allen RW. Numerical characterisation of folding flow microchannel mixers. *Chem Eng Sci*. 2007;62:2718–2727.
16. Aref H. Stirring by chaotic advection. *J Fluid Mech*. 1984;143:1–21.
17. Aref H. The development of chaotic advection. *Phys Fluids*. 2002;14:1315–1325.
18. Ottino JM, Wiggins S. Foundations of chaotic mixing 1. *Phil Trans R Soc Lond A*. 2004;362:937–970.
19. Brenner H. Dispersion resulting from flow through spatially periodic porous media. *Phylos Trans Roy Soc Lond*. 1980;297:81–133.
20. Vikhansky A. Lattice-Boltzmann method for yield-stress liquids. *J Non-Newtonian Fluid Mech*. 2008;155:95–100.
21. Vikhansky A. Coarse-grained simulation of chaotic mixing in laminar flows. *Phys Rev E*. 2006;73:056707.
22. Vikhansky A, Cox SM. Conditional moment closure for chemical reactions in laminar chaotic flows. *AIChE J*. 2007;53:19–27.

Manuscript received Sep. 15, 2009, and revision received Oct. 23, 2009.